Arabian Journal of Chemistry (2023) **16**, 104994

King Saud University

Arabian Journal of Chemistry

www.ksu.edu.sa
www.sciencedirect.com

ORIGINAL ARTICLE

Dehydrocostus lactone inhibits the proliferation and metastasis of hepatocellular carcinoma cells via modulating p53-p21-CDK2 signaling pathway

Yingying Tian [a,1], Beibei Ma [b,1], Xinyue Zhao [a], Shiqiu Tian [a], Yilin Li [a], Hailuan Pei [a], Shangyue Yu [a], Chuang Liu [a], Zhaozhou Lin [b,*], Zeping Zuo [b,*], Zhibin Wang [a,b,*]

[a] *School of Chinese Materia Medica, Beijing University of Chinese Medicine, Beijing 100029, China*
[b] *Research Institute of Beijing Tongrentang Co. LTD, Beijing 100079, China*

Received 13 December 2022; accepted 10 May 2023
Available online 16 May 2023

KEYWORDS

Dehydrocostus lactone (DL);
hepatocellular carcinoma (HCC);
Proliferation;
Apoptosis;
Metastasis;
p53-p21-CDK2

Abstract *Background:* Hepatocellular carcinoma (HCC), a malignancy with high mortality and recurrence rates, has very limited options for treatment strategies. Dehydrocostus lactone (DL) is the principal quality marker extracted from *Aucklandia lappa* Decne. and has been demonstrated to possess excellent anticancer activity. The key purpose of this study was to explore the therapeutic effects and potential mechanisms of DL on HCC.

Methods: The effect of DL on the cell viability of HCC cell lines (HepG2 and SK-HEP-1) and normal human hepatocyte cell line (L-O2) was examined by CCK8, colony formation, and BeyoClick^{TM}EdU-488 assays; Hoechst 33,258 staining and flow cytometry were utilized to determine the impact of DL on apoptosis; the sensitivity of HCC cells to DL was explored by adding Z-VAD-fmk. In addition, the expression of apoptosis-related proteins Bax, Bcl-2, and PARP was detected by western blotting; the expression of p-H2AX was investigated by western blotting and immunofluorescence staining; cell cycle distribution was observed using flow cytometry; the migration ability and invasiveness of HCC cells were assessed by wound healing assay and transwell assay; immunoblotting was applied to visualize the levels of EMT markers in the two HCC cell lines. Transcriptome sequencing was performed to reveal the underlying mechanisms of DL antitumor; western blotting and qRT-PCR were employed to verify the mRNA and protein abundance

* Corresponding authors.
E-mail addresses: linzhaozhou@yeah.net (Z. Lin), zepingzuo@126.com (Z. Zuo), wangzhibin4804@126.com (Z. Wang).

[1] These authors contributed equally to this work and shared the first authorship.

Peer review under responsibility of King Saud University.

Production and hosting by Elsevier

https://doi.org/10.1016/j.arabjc.2023.104994

of p53, p21, and CDK2; HepG2 xenograft in mice was used to test the anti-tumor effects of DL *in vivo*.

Results: DL suppressed the proliferation of HCC cell lines (HepG2 and SK-HEP-1) but had little effect on a normal human liver cell line (L-O2). In addition, DL also induced apoptotic death of the HCC cells by activating Bax and downregulating Bcl-2. The antiproliferative effects of DL could be attributed to increased DNA damage and G1-phase cell cycle arrest. Moreover, DL inhibited HCC cell invasiveness and migration *in vitro* by decreasing the levels of β-catenin, N-cadherin, and TCF8/ZEB1, and increasing the E-cadherin level. RNA sequencing indicated that DL exerted its anti-hepatoma effects partly via regulation of p53-p21-CDK2 signaling. These results were validated by our *in vivo* experiments, in which DL markedly suppressed the growth of HepG2 xenografts in a mouse model without any toxic side effects, which corresponded to decreased expression of Ki67 and MMP9 in the tumor tissues.

Conclusion: DL has significant anti-cancer effects in both *in vivo* and *in vitro* HCC models, and therefore could be further developed as a promising drug for the treatment of HCC.

1. Introduction

As reported by the World Health Organization, liver cancer ranks fifth in incidence among all fatal malignancies worldwide today and is the second leading cause of cancer-related deaths (Bray et al., 2018; Pei et al., 2023). As the most common subtype of primary liver cancer, hepatocellular carcinoma (HCC) accounts for about 70–90% of all hepatic cancer cases (Gao et al., 2020; Li et al., 2022). It is highly aggressive, poorly cured, and exhibits extremely high recurrence and mortality rates, resulting in most patients being diagnosed at an advanced stage with a very short remaining survival time of 6–20 months (Desai and Prasad, 2021). The presence of various risk factors in the general population, such as the high rate of hepatitis B/C virus infection, and the occurrence of chronic liver disease caused by excessive alcohol and tobacco addiction, pose serious challenges to the prevention and treatment of HCC (Feng et al., 2019; McGlynn et al., 2021; Sun et al., 2020). Traditional therapies for HCC including surgical resection, chemotherapy, and radiotherapy are not suitable for late-stage patients with metastasis and lymph node involvement as well as destroying the local organs, leaving a worse prognosis (Demir et al., 2021; Dobson, 2014). Meanwhile, the resistance and adverse effects of immunotherapeutic drugs like PD1/PDL1 monoclonal antibodies and targeted agents as tyrosine kinase receptor agonists cannot be ignored (Dai et al., 2022; Wang et al., 2023). Hence, it has been imperative to seek high-efficiency, low-toxicity and multi-targeted anti-HCC pharmaceuticals (Alibolandi et al., 2016; Ghadiri et al., 2017; Mottaghitalab et al., 2015).

Aucklandia lappa Decne. is a natural Chinese herbal medicine extensively used in various ethnic areas, which has a long-term historical accumulation and unique medical value (Cai et al., 2022). As far as investigations are concerned, *Aucklandia lappa* Decne. was originally recorded in the *Shen Nong Ben Cao Jing* (Chen et al., 2022), a classical medical literature of the Chinese nation, and was classified as one of the top-grade herbs, which was frequently used by the ancient Chinese people as one of the members of the Chinese medicine prescriptions for the treatment of many kinds of cancer because of its efficacy in dispersing stagnated hepatoqi and promoting qi circulation to relieve pain (Song et al., 2022; Zhang et al., 2021). Furthermore, modern pharmacological studies have demonstrated that *Aucklandia lappa* Decne. provides favorable therapeutic effects and safety for diseases including ulcerative colitis, breast carcinoma, cervical cancer, and benign prostatic hyperplasia (Chen et al., 2022; Choi et al., 2021; Hasson et al., 2018), as well as exhibiting excellent antioxidant, anti-apoptotic, anti-tumor, and anti-allergic properties (Lim et al., 2020; Seo et al., 2015; Zhou et al., 2020). More noticeably, Huang et al. had discovered that *Aucklandia lappa* Decne. could synergistically enhance the efficacy of gefitinib in the treatment of non-small cell lung cancer by directly exerting suppression of the EGFR signaling pathway (Huang et al., 2017).

As one of the natural sesquiterpene lactones extracted from *Aucklandia lappa* Decne., dehydrocostus lactone (DL) is a principal quality marker prescribed by the *Chinese Pharmacopoeia*, and has been likewise winning widespread attention for its remarkable anti-cancer benefits (Li et al., 2020). Reportedly, not only can DL inhibit the growth of gastrinoma cancer cells through sub-G1 phase cell cycle block and mitochondrial membrane potential loss channels (Long et al., 2019), but also suppress the proliferation of human laryngeal carcinoma via PI3K/Akt/Bad and ERS signaling pathways (Long et al., 2019). However, the potential implications and mechanisms of DL on HCC are still not clearly elucidated.

In this study, we intended to investigate the potential intervention efficacy and mechanisms of DL against HCC. With the establishment of *in vitro* HCC cell models, the impacts of DL on HCC cells proliferation and metastasis were inspected by means of western blotting, flow cytometer, immunofluorescence, and RNA sequencing. Furthermore, as an *in vivo* validation, the inhibitory effectiveness of DL on tumor growth was examined using HepG2 xenograft mice. In fact, the present study could contribute a novel perspective for mechanism excavation and deeper exploitation for DL.

2. Materials and methods

2.1. Culturing of malignant and normal human liver cell lines

HepG2 and L-O2 (a noncancerous human liver cell line) were acquired from American Type Culture Collection (VA, USA). SK-HEP-1 cells were obtained from the Cell Culture Center of the Institute of Basic Medical Sciences of the Chinese Academy of Medical Sciences (Beijing, China). We utilized Roswell Park Memorial Institute (RPMI)-1640, Dulbecco's modified Eagle medium (DMEM) and minimum essential medium (MEM) plus 10% fetal bovine serum (FBS) and 1% penicillin–streptomycin (P-S) solution for maintaining L-O2, HepG2 and SK-HEP-1 cell lines, respectively, in a 37 °C incubator filled with 5% CO_2.

2.2. Reagents and antibodies

Dehydrocostus lactone (DL) (purity, ≥ 98%; molecular weight, 230.30; formula, $C_{15}H_{18}O_2$) was obtained from

Chendu Must Bio-Technology Co. Ltd. (see Fig. 1A for its structure). The DMEM, MEM, and P-S solution were purchased from Gibco (CA, USA), and 0.25% trypsin and FBS were from Sigma (MO, USA). Matrigel and The Transwell chambers and matrigel were procured from Corning (NY, USA). The E.Z.N.A.® Total RNA Kit was obtained from Omega Bio-Tek (GA, USA), and the kits for EdU cell proliferation assay, Annexin V-FITC staining, and cell cycle analysis were from Biyuntian Biotechnology (Shanghai, China). Z-VAD-FMK (HY-16658B) and CVT-313 (HY-15339) were purchased from MedChem Express (NJ, USA). Antibodies specific for β-actin (4970 T), Bax (41162S), Bcl-2 (15071 T), PARP (9532 T), γ-H2AX (9718 T), E-cadherin (3195 T), N-cadherin (13116 T), TCF8/ZEB1 (3396 T), β-catenin (8480 T), p53 (2527 T), p21 (2947 T), p27 (3686 T) and CDK2 (18048 T), and horseradish peroxidase-conjugated goat anti-rabbit (7074P2) and anti-mouse (7076P2) IgG were obtained from Cell Signaling Technology (MA, USA). The enhanced chemiluminescence kit for developing target bands in Western blotting was procured from GE Healthcare.

2.3. Cell viability assay

Briefly, 3000 cells were filled into 100 μL cell culture medium in each well of 96-well plates and allowed to attach for 24 h. After treatment with DL (at concentrations of 0, 5, 10, 15, 20, and 25 μM) for varying durations (24 h and 48 h), the cells were subjected to a 2 h incubation in the Cell Counting Kit-8 (CCK-8) reagent. Afterwards, we utilized a microplate reader to record the 450 nm optical absorbance for each well.

2.4. Colony formation assay

Briefly, cells (3000 cells per well) were inoculated into 6well plates. The cell culture medium was refreshed 24 h later and added with 5 μM DL. After culturing the cells for 12 days, they were rinsed with phosphate-buffered saline (PBS), fixed inside 4% paraformaldehyde for 15 min, and subjected to crystal violet staining for 0.5 h. Colonies larger than 0.5 mm were counted.

2.5. Cell proliferation analysis using EdU

The cells were plated and cultured for 24 h in 96-well plates, followed by incubation with DL (0, 5, 10, and 15 μM) for 48 h. After aspirating 50 μL medium from each well, the same volume of EdU-containing medium (20 μg/mL) was supplemented to incubate the cells for two hours under 37 °C. The EdU-labeled proliferating cells were detected with the Beyotime BeyoClick™ EdU Cell Proliferation Kit (Shanghai, China) following the provider's instructions, and photographed and analyzed under a high-content screening (HCS) analysis system (Operetta CLS, PerkinElmer, USA).

2.6. Hoechst 33,258 staining

Eighty thousand cells were inoculated into each well of 6well plates, incubated for 24 h, and then subjected to DL treatments (0, 5, 10, and 15 μM). After incubating the cells with DL for 48 h, the cells were fixed for 10 min inside 4% paraformaldehyde and stained for 0.5 h by Hoechst 33,258 (10 μg/mL) at ambient temperature without being exposed to light. An Olympus IX73 fluorescence microscope (Japan) was utilized for observing and capturing the images.

2.7. Apoptosis and cell cycle assays

Cells were treated with DL as described above. Then the cells were analyzed for apoptosis with a Beyotime Annexin V-FITC kit (Shanghai, China) as per the protocol of the kit. For cell cycle assay, the cells were allowed to grow for 12 h in a medium without serum, incubated for 48 h with 10 μM DL, and analyzed by a kit for apoptosis and cell cycle assays from Beyotime (Shanghai, China) following the manual provided by the manufacturer.

2.8. Immunohistochemistry (IHC)

Cells maintained in 96-well plates were subjected to a 24 h treatment with 10 μM DL. After that, the cells were subjected to fixation with formaldehyde (4%) and then permeabilization using Triton X-100 (0.1%) for 10 and 20 min, respectively. The cells were then blocked for 1 h in 5% bovine albumin, incubated using an anti-γ-H2AX (Ser 139) antibody overnight at 4 °C, rinsed by PBS, and incubated for one hour using a DyLight 594-conjugated secondary antibody, followed by DAPI for 10 min. Images were acquired with High Content Screening (Operetta CLS, PerkinElmer, USA) using a 63 × water objective.

2.9. Wound healing assay

The cells were digested and inoculated into 12-well plates, and when their fusion grew to 90%, the cells were starved with serum-free medium for 12 h. After starvation for 12 h, scratch wounds were created on the HCC cell monolayers using 10 μL pipette tips. After the removal of dislodged cells, a serum-free medium containing 3 or 6 μM DL was added. The wound region was determined under a microscope at 0, 12, and 24 h after the addition of DL to appraise the HCC cells' migration ability.

2.10. Matrigel transwell invasion assay

Serum-free medium was utilized for starvation treatment of cells for 12 h, then digested into a single cell suspension and adjusted the density of the cells to 1 × 106/mL. We added to the upper chamber of Matrigel-coated transwell inserts with 200 μL drug supplemented serum-free medium containing 2 × 105 cells, and lower chambers added 750 μL medium with 10% FBS, respectively. The cells were maintained in the transwell set for 24 h and then those moved across the Matrigel were sequentially fixed for 5 min and 15 min by paraformaldehyde and methanol, respectively. Afterwards, these cells were subjected to crystal violet staining for 10 min, rinsed with PBS, and counted.

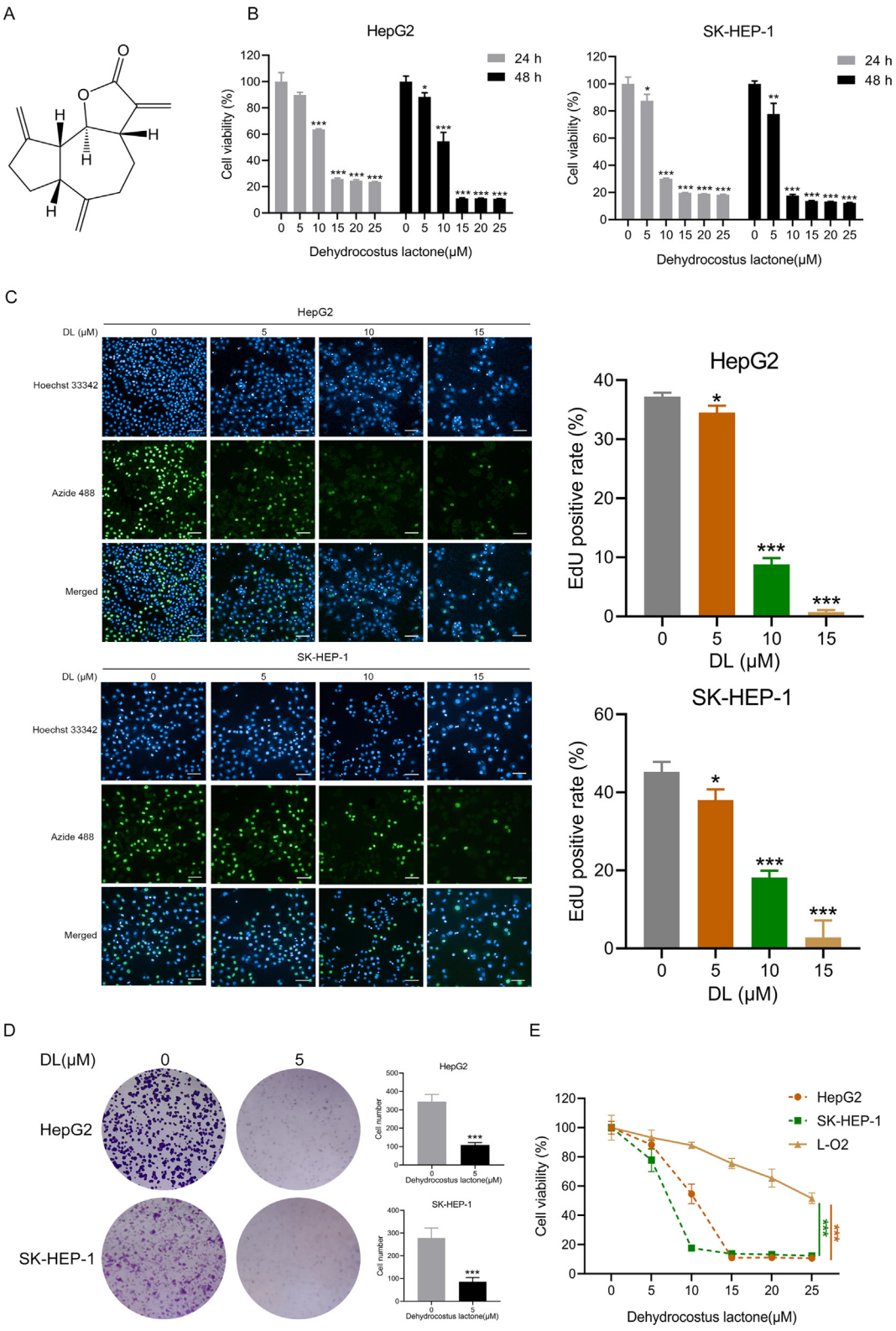

Fig. 1 DL repressed HCC cell proliferation. (A) The structure of DL. **(B)** Viability of the two HCC cell lines incubated with DL for 24 and 48 h. **(C)** Representative fluorescence images of HCC cells incubated for 24 h with 5, 10, and 15 μM DL and stained by BeyoClick™EdU-488 (20 × water lens, NA 1.0). The right panel indicates the EdU-positive proportion. **(D)** Representative images of colonies formed by the HCC cells treated with 5 μM DL for 12 days. **(E)** Viability of the HCC cells and normal hepatocytes following incubation for 48 h with DL. $*P < 0.05$, $**P < 0.01$, $***P < 0.001$.

2.11. Quantitative real-time PCR (qRT-PCR)

We utilized the E.Z.N.A. ®Total RNA Kit and the PrimeScript RT Reagent Kit for extraction of total RNA from treated HCC cells and reverse transcription, respectively. All the experiments were performed as per the instructions of the provider Quantitative PCR was implemented with TransStart Tip Green qPCR Kit using 4 μL cDNA as the template. The sequences of qRT-PCR primers are:

CDK1 forward: 5′-AAACTACAGGTCAAGTGGTAGCC-3′,
CDK1 reverse: 5′- TCCTGCATAAGCACATCCTGA-3′;
CDK2 forward: 5′-CCAGGAGTTACTTC TATGCCTGA-3′,
CDK2 reverse: 5′-TTCATCCAGGGGAGGTACAAC-3′;
p53 forward: 5′- GAGGTTGGCTCTGACTGTACC-3′,
p53 reverse: 5′- TCCGTCCCAGTAGATTACCAC-3′;
CDKN1A forward: 5′-AAGTCAGTTCCTTGTG GAGCC-3′,
CDKN1A reverse: 5′-GGTTCTGACGGACATCCCCA-3′;
EAF2 forward: 5′-GGCAGAAGCTAGTCTAATG GACC-3′,
EAF2 reverse: 5′-TGTACTGTGTCATGGTAGGATGT-3′.

2.12. Western blotting

Cells with different DL treatments (5, 10, and 15 μM for 24 h) were homogenized with RIPA buffer, and the total cell lysates were heated for 10 min at 99 °C for denaturation on an electric heating block. The samples were subjected to SDS-PAGE for separation of proteins with different molecular weights and then the proteins were blotted onto PVDF membranes. Following incubation for 1.5 h in 5% skimmed milk in TBST solution at ambient temperature, the membranes were incubated overnight with the primary antibody (1:1000) at 4 °C. The blots were rinsed by TBST the following day and then immersed for 4 h in diluted (2000 ×) secondary antibody solutions at 4 °C. After rinsing by TBST 3 times for 10 min each, the bands were developed using xx and visualized with Odyssey FC (LI-COR, Germany).

2.13. In vivo subcutaneous xenograft

Four- to five-week-old male BALB/c nude mice were procured from Beijing Vital River Laboratory Animal Technology Co. Ltd., and subcutaneously inoculated with 3×10^6/200 μL HepG2 cells into the right posterior region. Once the tumors grew to a volume of 100 mm^3, we randomly allocated the mice into the PBS, low-dose DL (10 mg/kg), high-dose DL (20 mg/kg), and 5-fluorouracil (5-FU) groups ($n = 6$ each). DL and PBS were injected intraperitoneally every day, while 5-FU was administered on alternate days. The body weight of the mice was appraised every day. Besides, the length and width of the subcutaneous tumor was measured by using electronic vernier calipers, and the volume of tumor was determined with the equation: tumor volume = (length × width × width)/2. Following the treatment regimens, the mice were subjected to euthanization, and the tumor tissues and main organs were collected and fixed in 4% paraformaldehyde. H&E staining and immunohistochemical analysis were performed as per standard protocols. All experiments on mice strictly followed the Guide for the Care and Use of Laboratory Animals.

2.14. Statistical analysis

Analyses of statistical data were implemented with GraphPad Prism 8.0. The means ± standard deviations (SD) of data from two groups were compared with unpaired two-tailed *t* test; while the data from ≥ 3 groups were subjected to one-way analysis of variance. $P < 0.05$ was deemed to signify statistical significance.

3. Results

3.1. DL repressed HCC cell proliferation

Given that the unlimited proliferation of cells represents a hallmark of cancer progression, a majority of chemodrugs are designed to inhibit the proliferative capacity of tumor cells (Cardano et al., 2020). We treated SK-HEP-1 and HepG2 cells using DL at different concentrations (0–25 μM) for 24 and 48 h. As shown in Fig. 1B, DL significantly suppressed the proliferative capacity of the HCC cells dose- and time-dependently. Furthermore, the EdU incorporation assay revealed that DL markedly decreased the proportion of the EdU-labeled (green fluorescence) proliferating cells (Fig. 1C). Consistent with these results, DL treatment also significantly reduced the colony-forming ability of the HCC cells (Fig. 1D). In contrast, DL had little inhibitory effect on the normal hepatocyte L-O2 cell line (Fig. 1E), indicating that DL displayed selective cytotoxicity against the HCC cells.

3.2. DL promoted HCC cell apoptosis

Apoptosis was analyzed via Hoechst staining (Busto et al., 2015). The two HCC cell lines treated with DL displayed stronger fluorescence (Fig. 2A), which was indicative of higher apoptosis rates. Flow cytometry analysis showed that exposure to 15 μM DL significantly enhanced the percentages of HepG2 and SK-HEP-1 cells that underwent apoptosis to 53.88 ± 9.58% and 55.6 ± 5.57% respectively (Fig. 2C). In addition, Z-VAD-fmk, an inhibitor against caspases, reduced the sensitivity of the HCC cells to DL (Fig. 2B), indicating that human HCC cell apoptosis invoked by DL is triggered by the caspase signaling cascade. Consistent with this, DL treatment increased the protein level of Bax, and downregulated that of Bcl-2 in the HepG2 and SK-HEP-1 cells (Fig. 2D). Furthermore, DL also activated cleaved PARP, which plays a crucial role in apoptosis (Soldani and Scovassi, 2002). Taken together, DL attenuated HCC cell growth via triggering apoptosis.

3.3. DL caused DNA damage and G1 cell cycle arrest in human HCC cells

Based on the pro-apoptotic effects of DL, we hypothesized that DL may induce DNA damage, which ultimately causes cell cycle blockage and apoptotic cell death. As expected, cells

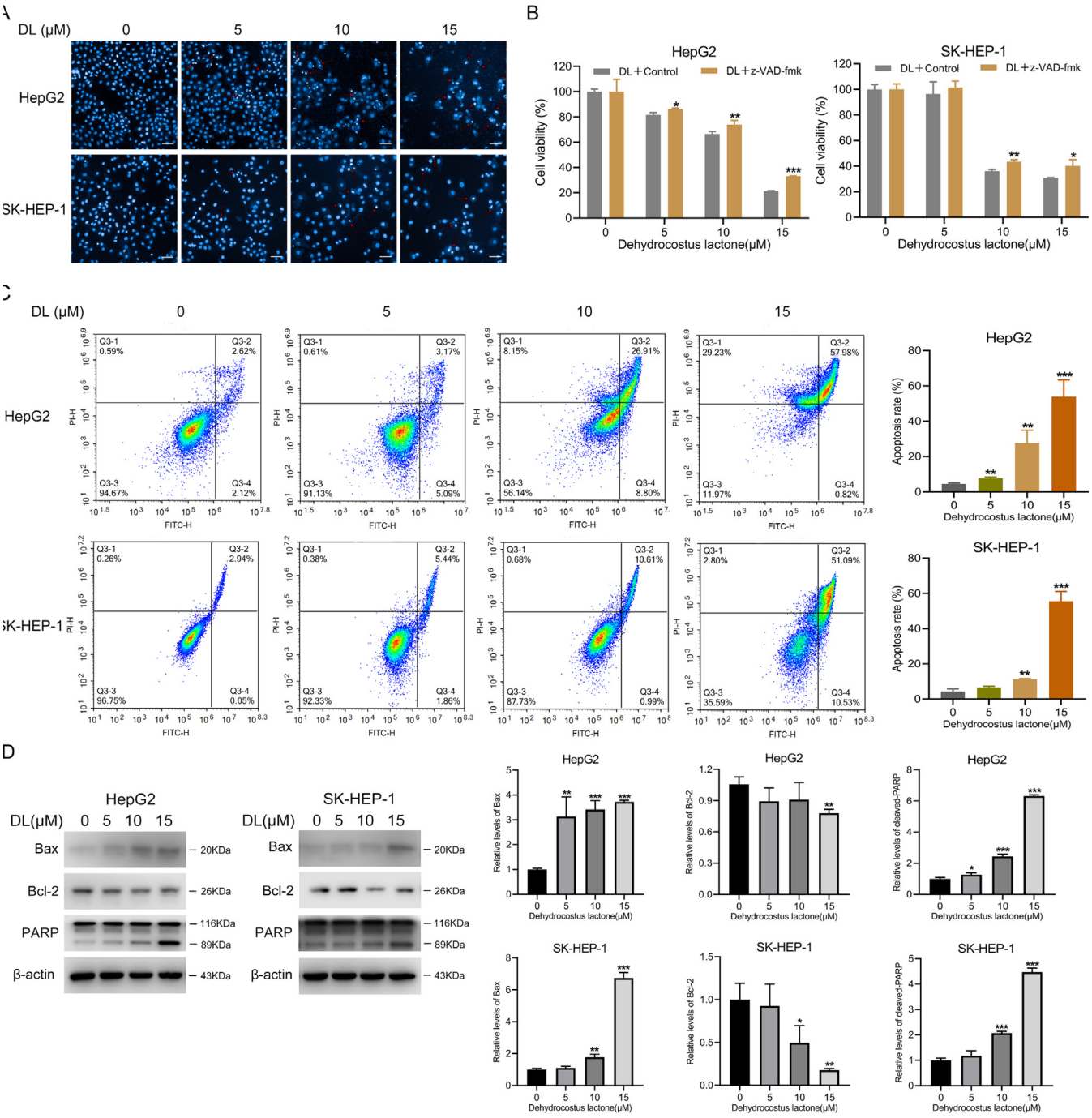

Fig. 2 DL invoked human HCC cell apoptosis. (A) Representative images of liver cancer cells incubated for 48 h with 0, 5, 10 and 15 μM DL and stained by Hoechst 33258. The apoptotic cells displayed blue fluorescence (20 × water lens, NA 1.0). **(B)** Viability of the two HCC cell lines incubated for 4 h with or without Z-VAD-fmk (5 μM) before treatment by various concentrations of DL for 24 h. **(C)** Flow cytometry plots showing percentage of apoptotic cells after DL treatment at various concentrations (0, 5, 10 and 15 μM) for 48 h. **(D)** Immunoblots showing Bcl-2 and Bax protein levels in cells treated for 24 h with DL (at concentrations of 0, 5, 10 and 15 μM). $*P < 0.05$, $**P < 0.01$, $***P < 0.001$.

treated with DL showed nuclear accumulation of γ-H2AX foci (Fig. 3A), which is indicative of DNA damage. In addition, DL significantly increased p-H2AX expression dose-dependently. (Fig. 3B). It was also exhibited that DL enhanced the proportion of G1-phase HCC cells, which suggests that it blocks cell cycle transition at the G1 stage (Fig. 3C).

3.4. DL attenuated the metastatic capacity of the HCC cells

As shown in the wound healing assay images in Fig. 4A, DL treatment reduced the coverage of the scratched region in the two HCC cell lines, suggesting that DL significantly reduced their migration ability. Furthermore, the number of HCC cells

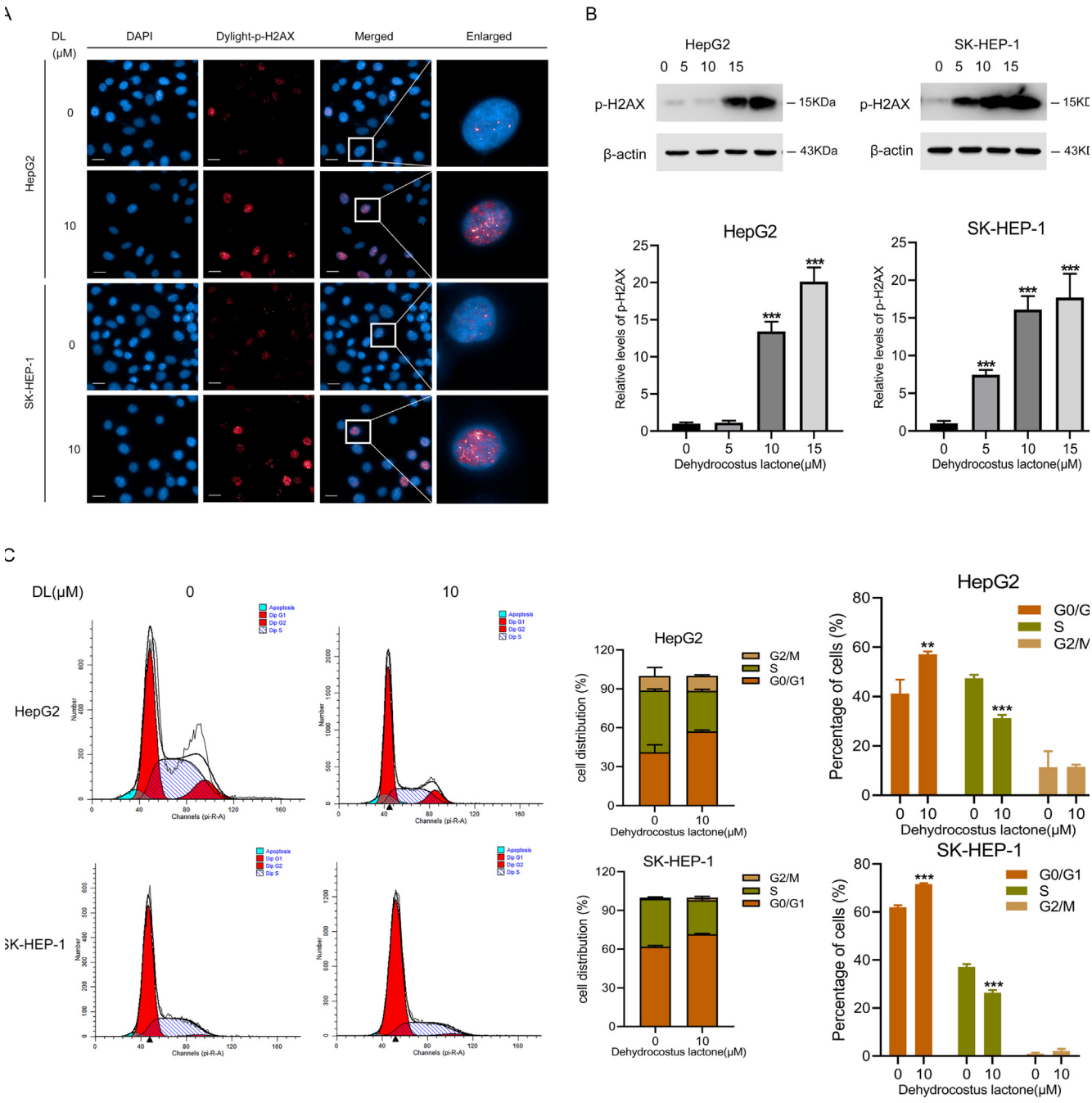

Fig. 3 DL induced damage of DNA and blockage of cell cycle at the G1 stage in human HCC cells. (A) Representative fluorescence images showing γ-H2AX foci in cells incubated with DL (10 μM) for 24 h (40 × water lens, NA 1.0). **(B)** Immunoblotting showing γ-H2AX levels in HCC cells subjected to 24-h-long DL treatments (at concentrations of 0, 5, 10 and 20 μM). **(C)** Flow cytometry plots showing the distribution of human HCC cells at different stages of cell cycle following treatment by 10 μM DL for 48 h. $^{**}P < 0.01$, $^{***}P < 0.001$.

that invaded through the Matrigel-coated membrane in Transwell assay also decreased when treated with DL (Fig. 4B), suggesting DL can also inhibit the invasiveness of HCC cells. The metastasis of malignant tumor cells is driven by the embryonic epithelial-to-mesenchymal (EMT) program (Cho et al., 2019). DL upregulated E-cadherin, the epithelial markers and decreased the expression of mesenchymal markers, including N-cadherin, β-catenin and TCF8/ZEB1 in the HCC cells (Fig. 4C), revealing that DL suppressed the EMT of human liver cancer cells.

3.5. The regulatory role of Dehydrocostus lactone on the p53-p21-CDK2 signaling pathway

To gain further insights into the molecular mechanisms underlying the effects of DL, we analyzed the transcriptomes of the

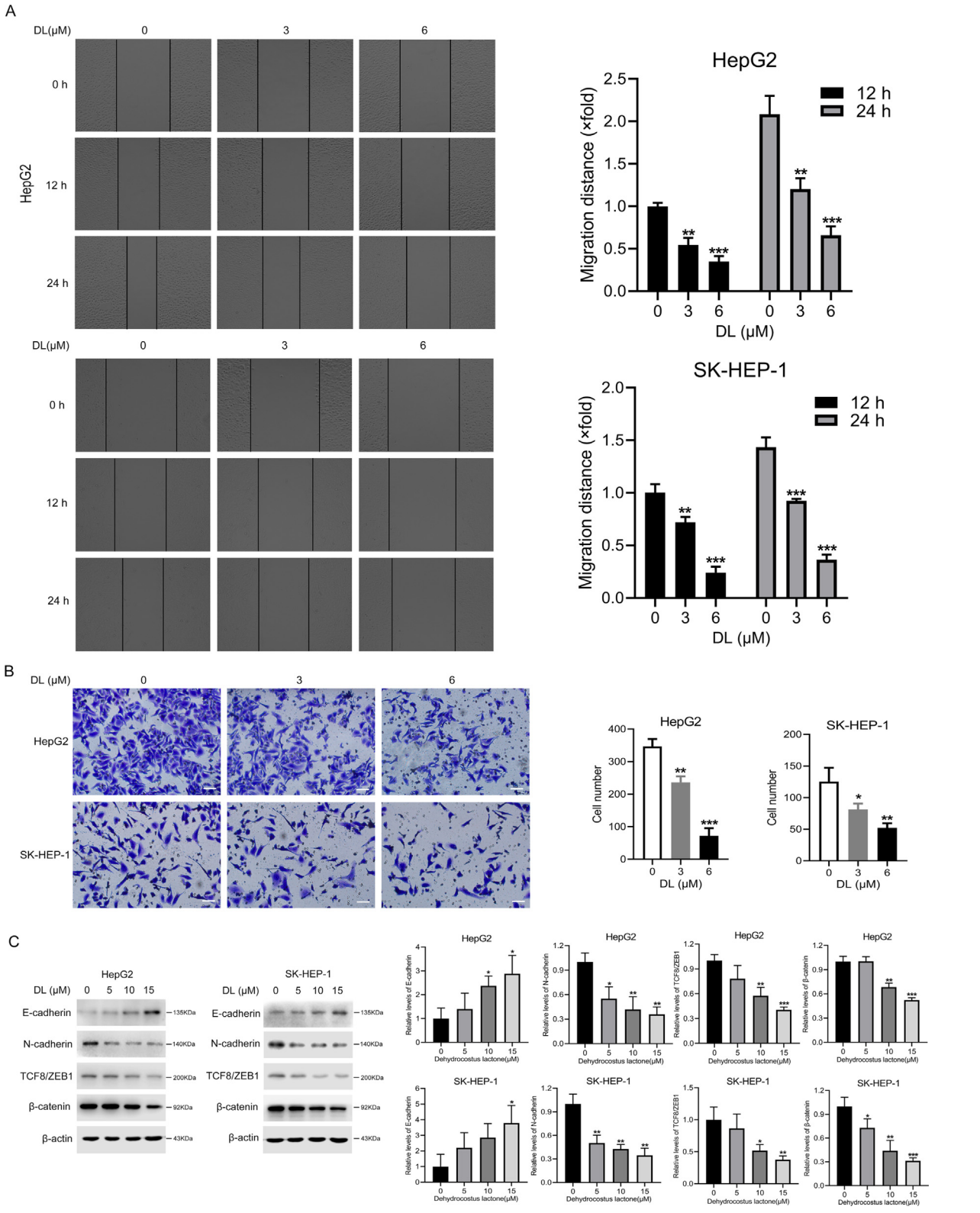

Fig. 4 DL suppressed the migration ability and invasiveness of HCC cells. (A) Representative pictures obtained from the wound healing assay showing the migration ability of the two HCC cell lines at 0, 12 and 24 h after treatment with 0, 3 and 6 μM DL (20 × magnification). (B) Representative images of transwell assay showing the invasion of cells through Matrigel 24 h after treatment with 0, 3 and 6 μM DL (20 × magnification). (C) Immunoblots showing levels of EMT markers in the two HCC cell lines treated as indicated. *, ** and *** indicate P values < 0.05, 0.01 and 0.001, respectively.

untreated and DL-treated HCC cells through RNA sequencing. As depicted in Fig. 5A, differential genes are enriched in cell cycle and p53 signaling pathway by data analysis. DNA damage always leads to p53-p21 pathway activation and blocks cell cycle progression at the G1 phase to allow the cells to repair the DNA lesions. The activation of p21 by p53 inhibits CDK2(He et al., 2005). In addition, the findings of qRT-PCR and Western blotting displayed that DL increased the mRNA and protein abundances of p53, p21 and reduced those of CDK2 in HepG2 and SK-HEP-1 cells (Fig. 5B, C). Taken together, the modulation of the p53-p21-CDK2 signaling cascade contributed in part to the anti-cancer effect of DL in human hepatoma cells. In addition, DL is also able to downregulate the mRNA abundance of CDK1 and upregulate that of EAF2 and the protein level of p27 (Fig. 5B, C).

3.6. Dehydrocostus lactone exerted tumoricidal efficacy in vivo.

To verify the results of *in vitro* experiments, we generated HepG2 cells-derived xenografts in BALB/c mice and injected different doses of DL into the mice for 22 days. As displayed by Fig. 6B, the average volume of tumors in mice injected with high-dose DL (20 mg/kg) was markedly lower compared to that of the PBS control mice. However, the body weight of the mice was not affected by DL treatment (Fig. 6A), which was indicative of the overall safety of DL. In addition, tumor tissues derived from the DL-treated mice exhibited a marked decrease in the in-situ expression of Ki67 and MMP9 compared to that of the control mice (Fig. 6D), indicating that DL can inhibit HCC cell proliferation and metastasis *in vivo*. Moreover, relative to the control, DL treatment also elevated the percentages of TUNEL-positive apoptotic cells in the tumor tissues (Fig. 6D). Finally, histopathological examination of the liver, heart, lung, kidney, and spleen tissues did not reveal any signs of toxicity due to DL treatment relative to the control group (Fig. 6C). Taken together, DL can effectively inhibit HCC growth *in vivo* with no detectable damage to major organs such as the heart, liver, spleen, lung and kidney.

4. Discussion

In recent years, the severe situation of HCC with restricted selective management and continuous attack on humans has forced the medical community to search for more reliable and innovative active drug precursors (Abedini et al., 2018; Domb et al., 2021). Under this circumstance, traditional Chinese medicine as a well-known complementary and alternative therapeutic strategy is opening up new avenues for HCC remedy. To the best of our knowledge, the extracts of chrysin from *Oroxylum indicum* (L.) Vent. (Rong et al., 2022), hypericin from *Hyperlcurn perforatum* L. (Choudhary et al., 2022), and baicalin from *Scutellaria baicalensis* Georgi have provided a more cutting-edge and scientific reference for the HCC pharmacotherapy (Hu et al., 2021). In this study, DL, screened from an everyday medicinal and edible herb, *Aucklandia lappa* Decne., has been reported in previous studies to have excellent anti-cancer activities. For example, DL could target IKKβ to inhibit NF-κB/COX-2 signaling pathway for ameliorating glioma(Wang et al., 2021b), as well as suppress Wnt/β-catenin pathway to antagonize colon carcinoma (Dong et al., 2015), and also trigger apoptosis in A549 lung cancer cell line (Hsu et al., 2009). Accordingly, the objective of present study is to credibly validate the curative efficacy of DL against HCC *in vitro* and *in vivo*, and further deeply elucidate its potential molecular anti-HCC mechanisms by multiple molecular biological means.

Most chemotherapeutic drugs inhibit malignant cell proliferation through blocking cell cycle or inducing apoptotic cell death (Gaglia et al., 2022). We found that DL significantly decreased the viability and proliferative capacity of the SK-HEP-1 and HepG2 cells, but had little impact on the non-malignant LO2 hepatocytes. Thus, DL exhibited selective cytotoxicity against HCC cells. Apart from uncontrolled proliferation, cancer cells are also characterized by their ability to bypass the apoptotic pathways. Therefore, many drugs have been developed that induce apoptosis directly or indirectly by increasing DNA damage (Mohammad et al., 2015; Wong, 2011). For instance, Ma et al. found that diosmetin (DIOS) promoted apoptosis of hepatoma cells through significantly suppressing the expression of Bcl-2 while promoting the expression of Bax, cleaved-caspases 3 and 8, cleaved-PARP, Bak, p53 and p21 (Ma and Zhang, 2020). Additionally, blocking cell cycle and causing DNA damage are also potent strategies for controlling cancer progression (Liu et al., 2023). DNA damage is characterized by the accumulation of γ-H2AX foci (Siddiqui et al., 2015), and triggers DNA repair, cell cycle arrest, and eventually cell death (Clay and Fox, 2021). Catechol, a natural plant-derived compound, increased γ-H2AX accumulation in the breast tumor-derived MCF-7 cells, resulting in blockage of cell cycle at the G1 stage through inhibition of cyclin E/Cdk2 mediated by p21. Moreover, p53 activation directly triggers caspase-dependent apoptosis via increasing the Bax/Bcl-2 ratio (Vazhappilly et al., 2021). Some metal-based anti-cancer agents exert their therapeutic effects through causing damage to DNA, and subsequently blockage of cell cycle at the G1 stage and apoptotic cell death (Wang et al., 2021a). In our study, DL enhanced the apoptosis rates of HCC cells via upregulating the protein levels of PARP and Bax, while downregulating that of Bcl-2. In addition, the inhibitory effect of DL on hepatoma cell growth was greatly weakened by the caspase inhibitor Z-VAD-fmk, which further supported the pro-apoptotic action of DL in liver cancer. Furthermore, there were significantly more γ-H2AX foci in the HCC cells after treatment by DL, which coincided with cell cycle arrest at G1 phase.

During HCC development, the malignant cells generally metastasize to several essential organs (Becker et al., 2014; Katyal et al., 2000). Therefore, metastasis suppression represents a useful therapeutic method for managing advanced HCC (Wan et al., 2013). During EMT, epithelial cells gradually lose contact inhibition, and become increasingly motile and invasive. This process is critical for tumor metastasis (Li et al., 2021). Yuan et al. showed that apigenin decreased the expression of the mesenchymal markers Snai1 and NF-κB in HCC cells, which reversed EMT, increased cell adhesion and decreased actin polymerization, eventually decreasing the migration and invasion capacity of the HCC cells (Qin et al., 2016). In our study as well, DL inhibited invasion and migration of the HCC cells *in vitro* by promoting the expression of E-cadherin, which is an epithelial marker, and repressing the expression of N-cadherin, TCF8/ZEB1 and β-catenin, which are mesenchymal markers. Likewise, DL treatment also

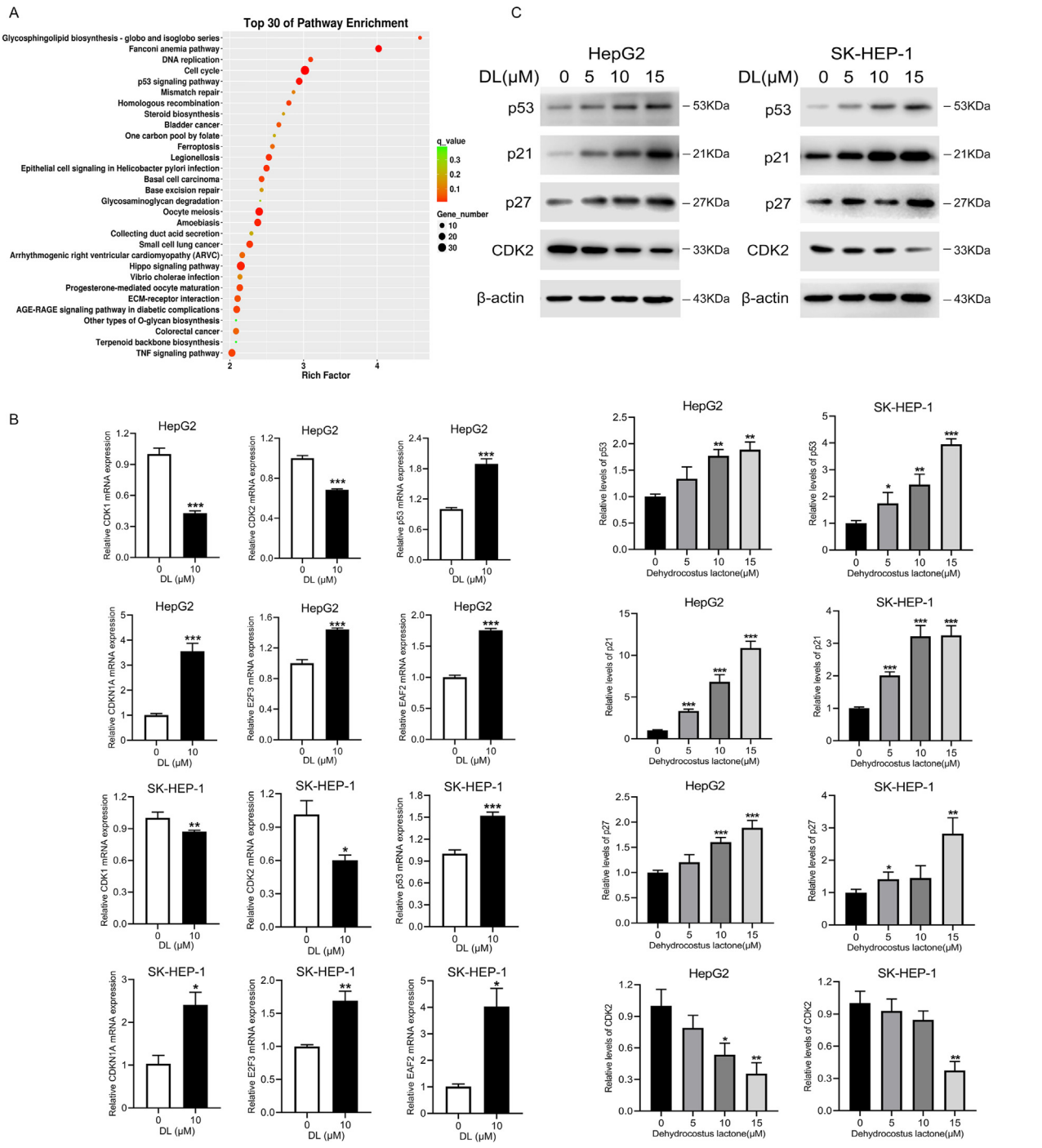

Fig. 5 DL can regulate the p53-p21-CDK2 signaling pathway to exert an anti-hepatic carcinoma effect. (A) Cells were subjected to a 24-h DL treatment at 10 μM and subsequently transcriptome sequencing. Transcriptome data analysis to identify enriched pathways. **(B)** Results of qRT-PCR showing p53, p21 and CDK2 mRNA levels in the HCC cells treated with DL (0 and 10 μM) for 24 h. **(C)** Immunoblots showing levels of p53, p21 and CDK2 proteins in HCC cells treated for 24 h with DL (0, 5, 10 and 20 μM). $*P < 0.05$, $**P < 0.01$, $***P < 0.001$.

decreased the expression of MMP9 in the xenografts *in vivo*. Thus, DL exhibits an anti-metastatic potential in HCC cells.

To further explore the molecular mechanisms for the effects of DL, we analyzed the transcriptomes of the control and DL-treated cells by RNA sequencing, and predicted the functions of the DEGs. The genes associated with the p53 pathway and cell cycle were significantly altered by DL treatment, and the results of RNA sequencing were validated by qRT-PCR and western blotting. These genes exert key mediating roles in DNA damage, apoptosis, and cell cycle (Armata et al., 2007; Meek, 2009). Dysregulation of CDK activity bypasses the key cellular checkpoints, resulting in unrestricted

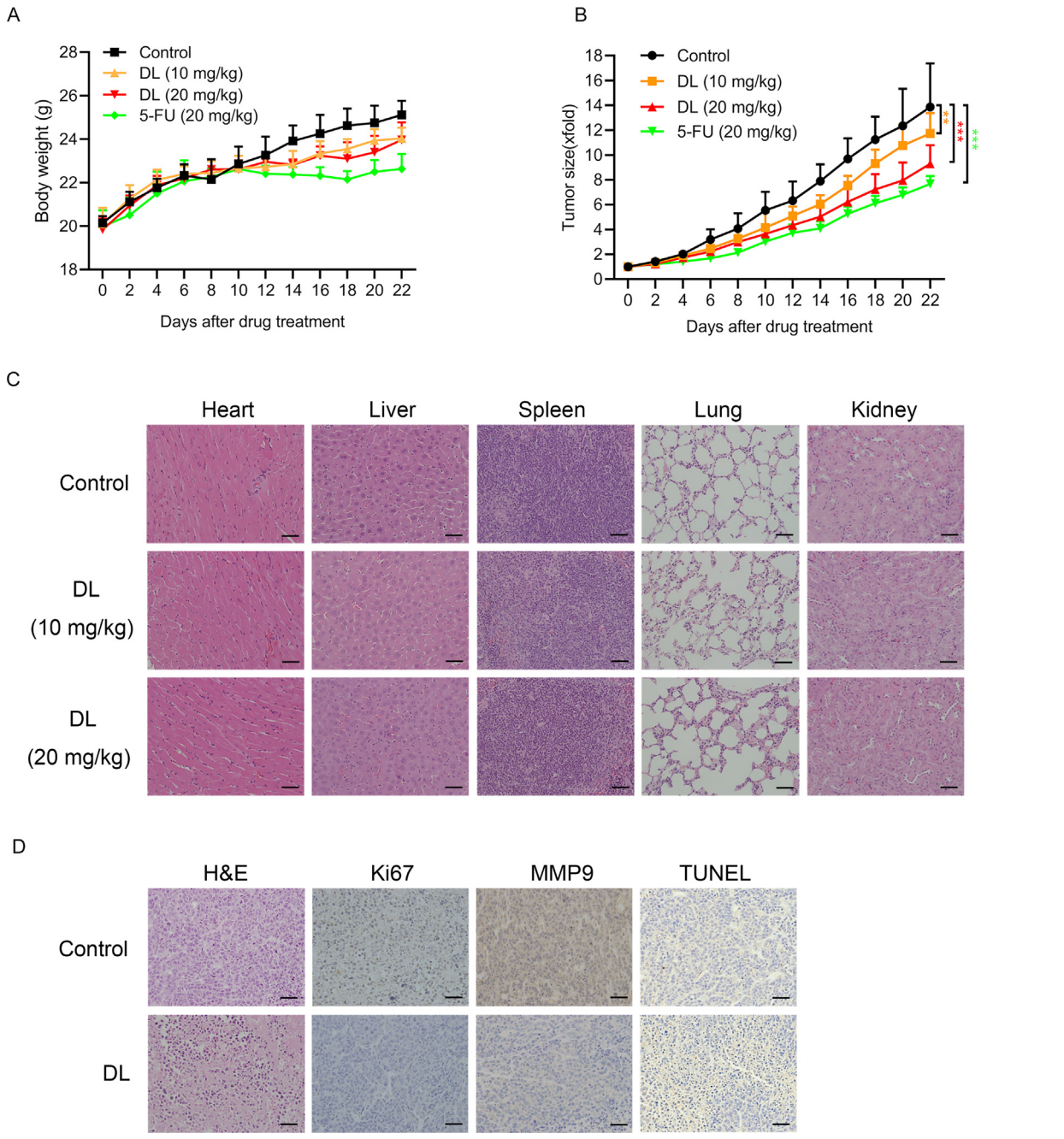

Fig. 6 DL inhibited the growth of HepG2 xenograft in mice. Each mouse was injected with 3×10^6 cells/0.2 mL HepG2 cells. Once tumor tissues grew to a volume of approximately 50 mm^3, the animals were treated with 10 and 20 mg/kg DL, PBS or 5-FU (20 mg/kg). The body weight **(A)** and tumor volume **(B)** of the mice were determined every two days. **(C)** Representative pictures of H&E-stained liver, heart, lung, kidney, and spleen tissues (20 × magnification). **(D)** Representative images of tumor tissues showing TUNEL-positive apoptotic cells and in-situ expression of Ki67 and MMP9 (20 × magnification).

cell proliferation and tumor growth. Thus, CDK1 and CDK2 are promising therapeutic targets for cancer (Brown et al., 2015). CDK1 and CDK2 regulate the progression of cell cycle from G1 to S phase, through the S phase, and from the G2 to M phase (Sakurikar and Eastman, 2016). P53 can suppress tumor development and regulate cell cycle progression, genome stability, apoptosis and senescence. The direct downstream target of p53 is p21/WAF1 (Engeland, 2018), also known as CDKN1A, which suppresses multiple CDKs and blocks cell cycle progression. Activation of p21 in tumor cells suppresses their ability to form colonies (El-Deiry, 2016). The ATM/ATR-CHK1/CHK2-p53-p21CIP1/WAF1-CDK axis functions as the G1 checkpoint in response to DNA damage (Chen and Poon, 2008). p27 induces G1 phase arrest by inhibiting CDK2/cyclinE (Balasubramanian et al., 1999). The cisplatin analogue 1R, 2R-diaminocyclohexane(*trans*-diacetato) (dichloro) platinumIV (DAP) forms DNA cross-links, which activates the DNA damage response, resulting

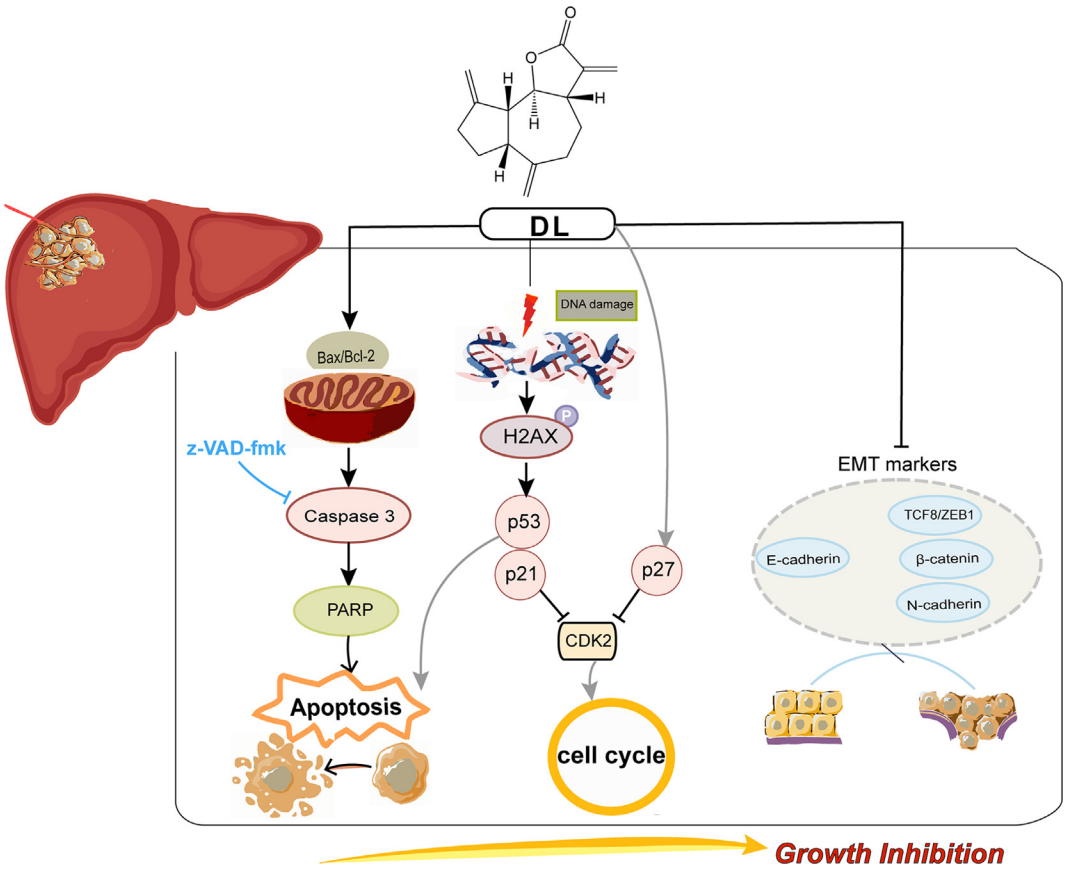

Fig. 7 **Schematic** presentation **of the anti-oncogenic effects of DL.** DL induced apoptosis and blockage of cell cycle at the G1 stage in the HCC cells via upregulating p53/p21 and p27, and downregulating CDK2. Moreover, DL inhibited the metastatic potential of the HCC cells partly via EMT blockade.

in G1-phase arrest via CDK suppression through the p53/p21 pathway (He et al., 2006). Yu et al. found that ginsenoside Rb1 (GRb1) repressed the cell cycle in tumor-bearing mice by activating the p53-p21-CDK2 axis (Yu et al., 2020). In our present study, DL repressed HCC cell growth through blocking cell cycle transition and triggering apoptosis via regulating the p53-p21-CDK2 pathway.

To summarize, DL inhibited HCC cell growth *in vitro* and *in vivo* through blocking cell cycle transition and triggering apoptosis via the p53-p21-CDK2 signaling channel, and suppressed their metastatic ability by blocking EMT (Fig. 7). Consequently, DL can undoubtedly be a promising pharmaceutical candidate for HCC prevention and has potential for further exploitation in the formulation of HCC treatment strategies. In the future, we will continue to thoroughly dissect the performance of DL intervention in diverse HCC model animals and investigate the perturbation of endogenous metabolic network caused by DL in the organism, so as to lay a sound foundation for the drug R&D journey of DL.

5. Conclusions

To sum up, our data revealed that DL suppressed the proliferative and metastatic capabilities of HepG2 and SK-HEP-1 cells, which are two HCC cell lines. These effects of DL were achieved through causing damage to DNA, blockage of cell cycle and apoptotic cell death. Additionally, DL inhibited hepatoma lesion development in a xenograft mouse model. Mechanistically, DL activated the p53/p21 pathway and downregulated epithelial-mesenchymal transition (EMT), which may be partially responsible for the DNA damage and the anti-oncogenic effects of DL. Consequently, our results unveil the possible mechanisms of action for DL, and establish an experimental basis for the development of its structural analogues for clinical applications.

CRediT authorship contribution statement

Yingying Tian: Methodology, Software, Data curation, Visualization, Writing – original draft. **Beibei Ma:** Methodology, Software, Data curation, Visualization, Writing – original draft. **Xinyue Zhao:** Formal analysis, Validation. **Shiqiu Tian:** Formal analysis, Validation. **Yilin Li:** Formal analysis, Validation. **Hailuan Pei:** Formal analysis, Validation. **Shangyue Yu:** Formal analysis, Validation. **Chuang Liu:** Formal analysis, Validation. **Zhaozhou Lin:** Conceptualization, Supervision. **Zeping Zuo:** Conceptualization, Supervision. **Zhibin Wang:** Conceptualization, Supervision.

Declaration of Competing Interest

The authors declare that they have no known competing financial interests or personal relationships that could have appeared to influence the work reported in this paper.

Acknowledgments

This research was funded by the National Science and Technology Major Project, grant number 2018ZX09201-011 and 2018ZX09301-011-003.

References

Abedini, F., Ebrahimi, M., Roozbehani, A.H., Domb, A.J., Hosseinkhani, H., 2018. Overview on natural hydrophilic polysaccharide polymers in drug delivery. Polym. Adv. Technol. 29, 2564–2573. https://doi.org/10.1002/pat.4375.

Alibolandi, M., Abnous, K., Sadeghi, F., Hosseinkhani, H., Ramezani, M., Hadizadeh, F., 2016. Folate receptor-targeted multimodal polymersomes for delivery of quantum dots and doxorubicin to breast adenocarcinoma: In vitro and in vivo evaluation. Int. J. Pharm. 500, 162–178. https://doi.org/10.1016/j.ijpharm.2016.01.040.

Armata, H.L., Garlick, D.S., Sluss, H.K., 2007. The ataxia telangiectasia-mutated target site Ser(18) is required for p53-mediated tumor suppression. Cancer Res. 67, 11696–11703. https://doi.org/10.1158/0008-5472.CAN-07-1610.

Balasubramanian, S., Kim, K.H., Ahmad, N., Mukhtar, H., 1999. Activation of telomerase and its association with G1-phase of the cell cycle during UVB-induced skin tumorigenesis in SKH-1 hairless mouse. Oncogene 18, 1297–1302. https://doi.org/10.1038/sj.onc.1202417.

Becker, A.K., Tso, D.K., Harris, A.C., Malfair, D., Chang, S.D., 2014. Extrahepatic metastases of hepatocellular carcinoma: a spectrum of imaging findings. Can. Assoc. Radiol. J.-JOURNAL DE L ASSOCIATION CANADIENNE DES RADIOLOGISTES 65, 60–66. https://doi.org/10.1016/j.carj.2013.05.004.

Bray, F., Ferlay, J., Soerjomataram, I., Siegel, R.L., Torre, L.A., Jemal, A., 2018. Global cancer statistics 2018: GLOBOCAN estimates of incidence and mortality worldwide for 36 cancers in 185 countries. CA-A Cancer J. Clin. 68, 394–424. https://doi.org/10.3322/caac.21492.

Brown, N.R., Korolchuk, S., Martin, M.P., Stanley, W.A., Moukhametzianov, R., Noble, M.E.M., Endicott, J.A., 2015. CDK1 structures reveal conserved and unique features of the essential cell cycle CDK. Nat. Commun. 6. https://doi.org/10.1038/ncomms7769.

Busto, N., Cano, B., Tejido, R., Biver, T., Leal, J.M., Venturini, M., Secco, F., Garcia, B., 2015. Aggregation features and fluorescence of Hoechst 33258. J. Phys. Chem. B 119, 4575–4581. https://doi.org/10.1021/jp512306c.

Cai, X., Yang, C., Qin, G., Zhang, M., Bi, Y., Qiu, X., Lu, L., Chen, H., 2022. Antimicrobial effects and active compounds of the root of Aucklandia Lappa Decne (Radix Aucklandiae). Front. Chem. 10. https://doi.org/10.3389/fchem.2022.872480.

Cardano, M., Tribioli, C., Prosperi, E., 2020. Targeting strategy to Proliferating Cell Nuclear Antigen (PCNA) as an effective strategy to inhibit tumor cell proliferation. Curr. Cancer Drug Targets 20, 240–252. https://doi.org/10.2174/1568009620666200115162814.

Chen, Y., Miao, Z., Sheng, X., Li, X., Ma, J., Xu, X., Li, H., Kang, A., 2022. Sesquiterpene lactones-rich fraction from Aucklandia lappa Decne. alleviates dextran sulfate sodium induced ulcerative colitis through co-regulating MAPK and Nrf2/Hmox-1 signaling pathway. J. Ethnopharmacol. 295. https://doi.org/10.1016/j.jep.2022.115401.

Chen, Y., Poon, R.Y.C., 2008. The multiple checkpoint functions of CHK1 and CHK2 in maintenance of genome stability. Front. Biosci.-Landmark 13, 5016–5029.

Cho, E.S., Kang, H.E., Kim, N.H., Yook, J.I., 2019. Therapeutic implications of cancer epithelial-mesenchymal transition (EMT). Arch. Pharm. Res. 42, 14–24. https://doi.org/10.1007/s12272-018-01108-7.

Choi, D.H., Kim, J.Y., An, J.H., Sung, S.H., Kong, H.S., 2021. Effects of Saussurea costus on apoptosis imbalance and inflammation in benign prostatic hyperplasia. J. Ethnopharmacol. 279. https://doi.org/10.1016/j.jep.2021.114349.

Choudhary, N., Collignon, T.E., Tewari, D., Bishayee, A., 2022. Hypericin and its anticancer effects: From mechanism of action to potential therapeutic application. Phytomedicine 105. https://doi.org/10.1016/j.phymed.2022.154356.

Clay, D.E., Fox, D.T., 2021. DNA Damage Responses during the Cell Cycle: Insights from Model Organisms and Beyond. Genes (Basel) 12. https://doi.org/10.3390/genes12121882.

Dai, B., Fan, M., Huang, X., Zhengyan, G., Cao, H., Hu, Y., Su, Q., Yang, T., Chen, Y., Peng, X., Liu, F., Zhang, Y., 2022. Shuanghua decoction exerts anticancer activity by activating NLRP3 inflammasome via ROS and inhibiting NF-?B signaling in hepatocellular carcinoma cells. Phytomedicine 103. https://doi.org/10.1016/j.phymed.2022.154249.

Demir, T., Lee, S.S., Kaseb, A.O., 2021. Systemic therapy of liver cancer, in: Sarkar, D., Fisher, P.B. (Eds.), Mechanisms and Therapy of Liver Cancer, Advances in Cancer Research. pp. 257–294. https://doi.org/10.1016/bs.acr.2020.12.001.

Desai, A., Prasad, V., 2021. Drug approvals in hepatocellular carcinoma-filling the nonexistent gap? JAMA Oncol. 7, 173–174. https://doi.org/10.1001/jamaoncol.2020.4811.

Dobson, J., 2014. Reducing the side effects of cyclophosphamide chemotherapy in dogs. Vet. Rec. 174, 248–249. https://doi.org/10.1136/vr.g1887.

Domb, A.J., Sharifzadeh, G., Nahum, V., Hosseinkhani, H., 2021. Safety Evaluation of Nanotechnology Products. Pharmaceutics 13. https://doi.org/10.3390/pharmaceutics13101615.

Dong, G., Shim, A.-R., Hyeon, J.S., Lee, H.J., Ryu, J.-H., 2015. Inhibition of Wnt/-Catenin pathway by dehydrocostus lactone and costunolide in colon cancer cells. Phytother. Res. 29, 680–686. https://doi.org/10.1002/ptr.5299.

El-Deiry, W.S., 2016. p21(WAF1) mediates cell-cycle inhibition, relevant to cancer suppression and therapy. Cancer Res. 76, 5189–5191. https://doi.org/10.1158/0008-5472.CAN-16-2055.

Engeland, K., 2018. Cell cycle arrest through indirect transcriptional repression by p53: I have a DREAM. Cell Death Differ. 25, 114–132. https://doi.org/10.1038/cdd.2017.172.

Feng, R.-M., Zong, Y.-N., Cao, S.-M., Xu, R.-H., 2019. Current cancer situation in China: good or bad news from the 2018 Global Cancer Statistics? Cancer Commun. 39. https://doi.org/10.1186/s40880-019-0368-6.

Gaglia, G., Kabraji, S., Rammosl, D., Dai, Y., Verma, A., Wang, S., Mills, C.E., Chung, M., Bergholz, J.S., Coyl, S., Lin, J.-R., Jeselsohn, R., Metzger, O., Winer, E.P., Dillon, D.A., Zhao, J.J., Sorger, P.K., Santagata, S., 2022. Temporal and spatial topography of cell proliferation in cancer. Nat. Cell Biol. 24, 316-+. https://doi.org/10.1038/s41556-022-00860-9.

Gao, Y.-X., Yang, T.-W., Yin, J.-M., Peng-Xiang, Y., Kou, B.-X., Chai, M.-Y., Liu, X.-N., Chen, D.-X., 2020. Progress and prospects of biomarkers in primary liver cancer (Review). Int. J. Oncol. 57, 54–66. https://doi.org/10.3892/ijo.2020.5035.

Ghadiri, M., Vasheghani-Farahani, E., Atyabi, F., Kobarfard, F., Mohamadyar-Toupkanlou, F., Hosseinkhani, H., 2017. Transferrin-conjugated magnetic dextran-spermine nanoparticles for targeted drug transport across blood-brain barrier. J. Biomed. Mater. Res. A 105, 2851–2864. https://doi.org/10.1002/jbm.a.36145.

Hasson, S.S., Al-Shubi, A.S.H., Al-Busaidi, J.Z., Al-Balushi, M.S., Hakkim, F.L., Rashan, L., Aleemallah, G.M., Al-Jabri, A.A., 2018. Potential of Aucklandia lappa Decne ethanolic extract to trigger apoptosis of human T47D and HeLa cells. Asian Pac. J. Cancer Prev. 19, 1917–1925. https://doi.org/10.22034/APJCP.2018.19.7.1917.

He, G., Kuang, J., Huang, Z., Koomen, J., Kobayashi, R., Khokhar, A.R., Siddik, Z.H., 2006. Upregulation of p27 and its inhibition of CDK2/cyclin E activity following DNA damage by a novel

platinum agent are dependent on the expression of p21. Br. J. Cancer 95, 1514–1524. https://doi.org/10.1038/sj.bjc.6603448.

He, G.G., Siddik, Z.H., Huang, Z.F., Wang, R.N., Koomen, J., Kobayashi, R., Khokhar, A.R., Kuang, J., 2005. Induction of p21 by p53 following DNA damage inhibits both Cdk4 and Cdk2 activities. Oncogene 24, 2929–2943. https://doi.org/10.1038/sj.onc.1208474.

Hsu, H.-F., Wu, Y.-C., Chen, L.-C., Houng, J.-Y., 2009. Induction of apoptosis of A549 lung cancer cell line by dehydrocostus lactone isolated from Glossogyne Tenuifolia. J. Food Drug Anal. 17, 107–115.

Hu, Q., Zhang, W., Wu, Z., Tian, X., Xiang, J., Li, L., Li, Z., Peng, X., Wei, S., Ma, X., Zhao, Y., 2021. Baicalin and the liver-gut system: Pharmacological bases explaining its therapeutic effects. Pharmacol. Res. 165. https://doi.org/10.1016/j.phrs.2021.105444.

Huang, G., Tong, Y.L., He, Q.D., Wang, J., Chen, Z.G., 2017. Aucklandia lappa DC. extract enhances gefitinib efficacy in gefitinib-resistance secondary epidermal growth factor receptor mutations. J. Ethnopharmacol. 206, 353–362. https://doi.org/10.1016/j.jep.2017.06.011.

Katyal, S., Oliver, J.H., Peterson, M.S., Ferris, J.V., Carr, B.S., Baron, R.L., 2000. Extrahepatic metastases of hepatocellular carcinoma. Radiology 216, 698–703. https://doi.org/10.1148/radiology.216.3.r00se24698.

Li, J., Liang, Q., Sun, G., 2021. Traditional Chinese medicine for prevention and treatment of hepatocellular carcinoma: A focus on epithelial-mesenchymal transition. J. Integrative Med.-JIM 19, 469–477. https://doi.org/10.1016/j.joim.2021.08.004.

Li, S., Pei, W., Yuan, W., Yu, D., Song, H., Zhang, H., 2022. Multi-omics joint analysis reveals the mechanism of action of the traditional Chinese medicine Marsdenia tenacissima (Roxb.) Moon in the treatment of hepatocellular carcinoma. J. Ethnopharmacol. 293. https://doi.org/10.1016/j.jep.2022.115285.

Li, Q., Wang, Z., Xie, Y., Hu, H., 2020. Antitumor activity and mechanism of costunolide and dehydrocostus lactone: Two natural sesquiterpene lactones from the Asteraceae family. Biomed. Pharmacother. https://doi.org/10.1016/j.biopha.2020.109955.

Lim, J.S., Lee, S.H., Lee, S.R., Lim, H.J., Roh, Y.S., Won, E.J., Cho, N., Chun, C., Cho, Y.C., 2020. Inhibitory effects of aucklandia lappa decne. Extract on inflammatory and oxidative responses in lps-treated macrophages. Molecules 25. https://doi.org/10.3390/molecules25061336.

Liu, H., Zhang, W., Jin, L., Liu, S., Liang, L., Wei, Y., 2023. Plumbagin exhibits genotoxicity and induces G2/M cell cycle arrest via ROS-mediated oxidative stress and activation of ATM-p53 signaling pathway in hepatocellular cells. Int. J. Mol. Sci. 24. https://doi.org/10.3390/ijms24076279.

Long, H.Y., Huang, Q.X., Yu, Y.Y., Zhang, Z.B., Yao, Z.W., Chen, H.B., Feng, J.W., 2019. Dehydrocostus lactone inhibits in vitro gastrinoma cancer cell growth through apoptosis induction, sub-G1 cell cycle arrest, DNA damage and loss of mitochondrial membrane potential. Arch. Med. Sci. 15, 765–773. https://doi.org/10.5114/aoms.2018.73128.

Ma, A., Zhang, R., 2020. Diosmetin Inhibits Cell Proliferation, Induces Cell Apoptosis and Cell Cycle Arrest in Liver Cancer. Cancer Manag. Res. 12, 3537–3546. https://doi.org/10.2147/CMAR.S240064.

McGlynn, K.A., Petrick, J.L., El-Serag, H.B., 2021. Epidemiology of hepatocellular carcinoma. Hepatology 73, 4–13. https://doi.org/10.1002/hep.31288.

Meek, D.W., 2009. Tumour suppression by p53: a role for the DNA damage response? Nat. Rev. Cancer 9, 714–723. https://doi.org/10.1038/nrc2716.

Mohammad, R.M., Muqbil, I., Lowe, L., Yedjou, C., Hsu, H.-Y., Lin, L.-T., Siegelin, M.D., Fimognari, C., Kumar, N.B., Dou, Q.P., Yang, H., Samadi, A.K., Russo, G.L., Spagnuolo, C., Ray, S.K., Chakrabarti, M., Morre, J.D., Coley, H.M., Honoki, K., Fujii, H., Georgakilas, A.G., Amedei, A., Niccolai, E., Amin, A., Ashraf, S. S., Helferich, W.G., Yang, X., Boosani, C.S., Guha, G., Bhakta, D., Ciriolo, M.R., Aquilano, K., Chen, S., Mohammed, S.I., Keith, W.N., Bilsland, A., Halicka, D., Nowsheen, S., Azmi, A.S., 2015. Broad targeting of resistance to apoptosis in cancer. Semin. Cancer Biol. 35, S78–S103. https://doi.org/10.1016/j.semcancer.2015.03.001.

Mottaghitalab, F., Farokhi, M., Ali, S.M., Atyabi, F., Hosseinkhani, H., 2015. Silk fibroin nanoparticle as a novel drug delivery system. J. Control. Release 206, 161–176. https://doi.org/10.1016/j.jconrel.2015.03.020.

Pei, T., Dai, Y., Tan, X., Geng, A., Shengrong, L.i., Gui, Y., Hu, C., An, J., Yu, X., Bao, X., Wang, D., 2023. Yupingfeng San exhibits anticancer effect in hepatocellular carcinoma cells via the MAPK pathway revealed by HTS2 technology. J. Ethnopharmacol. 306. https://doi.org/10.1016/j.jep.2023.116134.

Qin, Y., Zhao, D., Zhou, H., Wang, X., Zhong, W., Chen, S., Gu, W., Wang, W., Zhang, C., Liu, Y., Liu, H., Zhang, Q., Guo, Y., Sun, T., Yang, C., 2016. Apigenin inhibits NF-kB and snail signaling, EMT and metastasis in human hepatocellular carcinoma. Oncotarget 7, 41421–41431. https://doi.org/10.18632/oncotarget.9404.

Rong, W., Wan, N., Zheng, X., Shi, G., Jiang, C., Pan, K., Gao, M., Yin, Z., Gao, Z.-J., Zhang, J., 2022. Chrysin inhibits hepatocellular carcinoma progression through suppressing programmed death ligand 1 expression. Phytomedicine 95. https://doi.org/10.1016/j.phymed.2021.153867.

Sakurikar, N., Eastman, A., 2016. Critical reanalysis of the methods that discriminate the activity of CDK2 from CDK1. Cell Cycle 15, 1184–1188. https://doi.org/10.1080/15384101.2016.1160983.

Seo, C.S., Lim, H.S., Jeong, S.J., Shin, H.K., 2015. Anti-allergic effects of sesquiterpene lactones from the root of Aucklandia lappa Decne. Mol. Med. Rep. 12, 7789–7795. https://doi.org/10.3892/mmr.2015.4342.

Siddiqui, M.S., Francois, M., Fenech, M.F., Leifert, W.R., 2015. Persistent gamma H2AX: a promising molecular marker of DNA damage and aging. Mutation Res.-Rev. MUTATION RESEARCH 766, 1–19. https://doi.org/10.1016/j.mrrev.2015.07.001.

Soldani, C., Scovassi, A.I., 2002. Poly(ADP-ribose) polymerase-1 cleavage during apoptosis: an update. Apoptosis 7, 321–328. https://doi.org/10.1023/A:1016119328968.

Song, S.Y., Zhou, J.Y., Li, Y., Liu, J.T., Li, J.Z., Shu, P., 2022. Network pharmacology and experimental verification based research into the effect and mechanism of Aucklandiae Radix-Amomi Fructus against gastric cancer. Sci. Rep. 12. https://doi.org/10.1038/s41598-022-13223-z.

Sun, N., Teng, A., Zhao, Y., Liu, H., Tu, J., Jia, Q., Wang, Q., 2020. Immunological and anticancer activities of seleno-ovalbumin (Se-OVA) on H22-bearing mice. Int. J. Biol. Macromol. 163, 657–665. https://doi.org/10.1016/j.ijbiomac.2020.07.006.

Vazhappilly, C.G., Hodeify, R., Siddiqui, S.S., Laham, A.J., Menon, V., El-Awady, R., Matar, R., Merheb, M., Marton, J., al Zouabi, H.A.K., Radhakrishnan, R., 2021. Natural compound catechol induces DNA damage, apoptosis, and G1 cell cycle arrest in breast cancer cells. Phytother. Res. 35, 2185–2199. https://doi.org/10.1002/ptr.6970.

Wan, L., Pantel, K., Kang, Y., 2013. Tumor metastasis: moving new biological insights into the clinic. Nat. Med. 19, 1450–1464. https://doi.org/10.1038/nm.3391.

Wang, H., Wei, J., Jiang, H., Zhang, Y., Jiang, C., Ma, X., 2021a. Design, synthesis and pharmacological evaluation of three novel Dehydroabietyl Piperazine Dithiocarbamate Ruthenium (II) Polypyridyl Complexes as potential antitumor agents: DNA damage, cell cycle arrest and apoptosis induction. Molecules 26. https://doi.org/10.3390/molecules26051453.

Wang, C., Yang, L., Xu, S., Guo, H., Hewen, G., Wang, Q., Jiang, X., Fei, M., Zhang, J., 2023. Systematic analysis of the role and significance of target genes of active ingredients of traditional Chinese medicine injections in the progression and immune

microenvironment of hepatocellular carcinoma. Front. Pharmacol. 13. https://doi.org/10.3389/fphar.2022.1095965.

Wang, J., Yu, Z., Wang, C., Tian, X., Huo, X., Wang, Y., Sun, C., Feng, L., Ma, J., Zhang, B., Yang, Q., Ma, X., Xu, Y., 2021b. Dehydrocostus lactone, a natural sesquiterpene lactone, suppresses the biological characteristics of glioma, through inhibition of the NF-kappa B/COX-2 signaling pathway by targeting IKK beta (vol 7, pg 1270, 2017). Am. J. Cancer Res. 11, 979–981.

Wong, R.S.Y., 2011. Apoptosis in cancer: from pathogenesis to treatment. J. Exp. Clin. Cancer Res. 30. https://doi.org/10.1186/1756-9966-30-87.

Yu, S., Xia, H., Guo, Y., Qian, X., Zou, X., Yang, H., Yin, M., Liu, H., 2020. Ginsenoside Rb1 retards aging process by regulating cell cycle, apoptotic pathway and metabolism of aging mice. J. Ethnopharmacol. 255. https://doi.org/10.1016/j.jep.2020.112746.

Zhang, L.L., Xiao, Y., Yang, R.J., Wang, S.Y., Ma, S.X., Liu, J.L., Xiao, W., Wang, Y.H., 2021. Systems pharmacology to reveal multi-scale mechanisms of traditional Chinese medicine for gastric cancer. Sci. Rep. 11. https://doi.org/10.1038/s41598-021-01535-5.

Zhou, Q., Zhang, W.X., He, Z.Q., Wu, B.S., Shen, Z.F., Shang, H.T., Chen, T., Wang, Q., Chen, Y.G., Han, S.T., 2020. The possible anti-inflammatory effect of dehydrocostus lactone on DSS-Induced colitis in mice. Evid. Based Complement. Alternat. Med. 2020. https://doi.org/10.1155/2020/5659738.